Supporting Information for:

Tuning radical relay residues by proton management rescues protein electron hopping

Estella F. Yee[†], Boris Dzikovski[†,§], Brian R. Crane[†,*]

[†]Department of Chemistry and Chemical Biology, Cornell University, Ithaca, New York 14853, United States
[§]National Biomedical Center for Advanced ESR Technologies (ACERT), Cornell University, Ithaca, New York 14850, United States

The PDF file includes:

Materials and Methods

Protein Purification

Cytochrome c

The gene for wild-type yeast iso-1-Cc from *Saccharomyces cerevisiae* was expressed in *E. coli* BL21 (DE3) cells from a PBTR1 vector[1–3] that also contains the yeast heme lyase gene. Cells were grown in LB-Miller media for 20 h at 37 °C with 125 μg/mL ampicillin and 50 – 100 μg/mL Δ-aminolevulenic acid to improve heme incorporation. Harvested cells were resuspended in 50 mM sodium phosphate (NaPi), pH 8 and lysed by sonication. Lysate was centrifuged at 20,000 RPM for 1 h at 4 °C and the supernatant was directly loaded onto an equilibrated HiPrep CMFF 16/10 column (GE Healthcare). After washing with one column volume (40 mL) of 50 mM NaPi, a linear gradient of 50 mM NaPi, 500 mM sodium chloride (NaCl), pH 8, was applied over 100 mL to elute the bound protein. Protein fractions were pooled and further purified by size-exclusion chromatography (HiLoad Superdex 75 26/60; GE Healthcare). Colored fractions were combined, concentrated, aliquotted, and stored at –80 °C. Concentrations were measured at $Abs_{550\ nm} - Abs_{540\ nm}$, $\varepsilon = 19.2\ mM^{-1}\ cm^{-1}$.

Cytochrome c peroxidase

Cytochrome c Peroxidase (CcP) constructs from *Saccharomyces cerevisiae* were cloned into the ppSUMO pET28a-based vector to provide an N-terminal His-tag followed by a SUMO protein[1]. The vector was transformed into BL21(DE3) cells, which were then grown at 37 °C in LB-Miller media with kanamycin (50 μg/mL). Cells were induced with 100 μM isopropyl β-D-1-thiogalactopyranoside (IPTG; 25 μg/mL) once $O.D._{600}$ reached 0.8 – 1.2 and overexpressed at room temperature for ~18 h. Cells were harvested and resuspended in lysis buffer (50 mM HEPES, pH 7.0, 150 mM NaCl, and 5 mM imidazole). Cells were then lysed by sonication and centrifuged at 20,000 RPM for 1 h at 4 °C. CcP was purified by Ni-NTA resin (Qiagen) and concentrated. SUMO-His_6 tag was cleaved with ULP-1 protease and dialyzed into 100 mM potassium phosphate (KPi), pH 6, overnight at 4 °C. Eluent was flowed through a Ni-NTA column

to remove the tags. To improve heme incorporation, the eluent was incubated with one molar equivalent of hemin dissolved in 500 µL 0.1 M sodium hydroxide (NaOH) overnight at 4 °C. The reaction was quenched with an equal amount of 0.1 M acetic acid. Unreacted hemin and precipitated protein were removed by centrifugation at 13,000 RPM for 10 min. The soluble portion was purified by size-exclusion chromatography (HiLoad Superdex 75 26/60) in 100 mM KPi, pH 6. Protein fractions were combined and loaded directly onto an equilibrated HiPrep Q XL 16/10 column (GE Healthcare). A linear gradient of 500 mM KPi, pH 6, was applied over 160 mL to elute the protein and separate the apo-CcP from the Fe-CcP. All fractions with high heme incorporation ($Abs_{408\ nm}/Abs_{280\ nm} > 1$) were pooled, concentrated, aliquoted, and stored at –80 °C. All preparations of the enzyme conformed to the purity criteria previously described[4]. Concentrations were determined at 408 nm, $\varepsilon = 96\ mM^{-1}\ cm^{-1}$.

Site-directed Mutagenesis

Single residue substitutions in CcP were produced by the overlap extension PCR method on the CcP construct within the ppSUMO vector. For fluorotyrosine derivatives, site 191 was replaced with a TAG amber stop codon and the final termination codon with either a TAA or TGA stop codon.

Tyrosine phenol lyase

Tyrosine phenol lyase (TPL) in pET23b (generous gift from the Tonge lab, Stony Brook University) was overexpressed in BL21(DE3)pLysS cells (Novagen) in LB-Miller media with chloramphenicol (12 µg/mL) and ampicillin (50 µg/mL) at room temperature for 18 h. Cells were harvested, resuspended in lysis buffer (50 mM NaPi, pH 7, 150 mM NaCl, 5 mM DTT), and lysed by sonication. Cell detritus was removed by centrifugation at 20,000 RPM, 1 h, 4 °C, and the resulting lysate was purified by Ni-NTA resin. The eluted protein was then further purified by size-exclusion chromatography (HiLoad Superdex 75 26/60) in 50 mM NaPi, pH 7, 150 mM NaCl buffer. Protein fractions were pooled and glycerol added to a final percentage of 10% to aid in stability. Samples were stored at –80 °C and used within one week of preparation to avoid loss of activity. Final yield was ~200 mg per 8 L culture.

Fluorotyrosine preparation and purification

Fluorotyrosine amino acids were prepared as described[5,6]. Pyridoxal 5' phosphate and 2,6-difluorophenol were purchased from Oakwood Chemicals; 2,3,6-trifluorophenol was acquired from Alfa Aesar. (Note that the numbering changes when converting the fluorophenol into fluorotyrosine.) A 1-L solution of 30 mM ammonium acetate, pH 8, 60 mM sodium pyruvate, 40 μM pyridoxal 5' phosphate, and 50 mM β-mercaptoethanol was prepared and filtered through a 0.22 μm filter into a bottle. To this solution, 10 mM fluorophenol was added while adjusting the final pH to 8. Approximately 150 units (~80 mg) of purified TPL were added to the mixture drop-wise while stirring, after which, the reaction was covered in foil and continually stirred at room temperature. Every two days, 30 units (~16 mg) of TPL were added to the reaction mixture for a total of ~1 week. The mixture was quenched by acidification to pH ~2.5, and precipitated protein was removed by filtration or centrifugation. The solution was extracted twice with 500 mL of ethyl acetate to remove unreacted phenols. The aqueous layer was run through a column (inner diameter ~4 in) of activated Dowex 50W-X8 (50 – 100 mesh; Beantown Chemical Corporation) equilibrated in Nanopure water. The column was washed with 1 L of filtered Nanopure water to remove impurities, and the fluorotyrosine amino acids were eluted with 10% ammonium hydroxide in ~7 mL fractions. Fractions were spotted on a silica thin-layer chromatography plate and visualized by ninhydrin stain (0.19% (w/v) ninhydrin, 95% ethanol, 0.5% acetic acid, 4.5% water). Fractions containing the amino acid were combined, concentrated by roto-evaporation, and lyophilized to dryness. Fluorotyrosine products were confirmed by ^{1}H NMR and ^{19}F NMR in D_2O[6]. Yield: ~50%.

Fluorotyrosine incorporation into site 191 of CcP

BL21(DE3) cells were co-transformed with ppSUMO containing the gene for CcP (with site 191 replaced by TAG in ppSUMO) and with a pEVOL system expressing the E3 aminoacyl-tRNA synthetase (generous gift from the Stubbe group, MIT)[7]. Cells were grown in LB-Miller media with kanamycin (25 μg/mL) and chloramphenicol (12 μg/mL) at 37 °C until they reached an $O.D._{600}$ of ~0.4, after which 1 mM of the fluorotyrosine dissolved in 0.1 M NaOH was added to the culture and incubated for 10 minutes. Subsequently, E3 expression was induced with 0.05%

(w/v) arabinose. After 1 h, CcP production was induced with 100 µM IPTG, and cells were grown at 37 °C for 18 h. Cells were harvested and purified similarly as other CcP variants.

Experimental Procedures

Single and multiple turnover measurements

Single turnover measurements were conducted with 1800 µL of 1 µM CcP and 2 µM reduced Cc in 100 mM KPi, pH 6 buffer at 20 °C. Reactions were initiated by rapidly adding 3 – 4 µL of H_2O_2 stock to a final concentration of 2 µM while stirring at 700 RPM (Hewlett-Packard 89090A Peltier). Moderately high ionic strength[1,8] and constant stirring[9] allows for substantial preformed complex, prevents second-site binding, and increases Cc off-rates. The rate of Cc(Fe^{2+}) oxidation was monitored at the heme Q bands $Abs_{550\ nm}$–$Abs_{540\ nm}$ and the CcP oxy-ferryl species at $Abs_{434\ nm}$ (a Cc (Fe^{2+}/Fe^{3+}) isosbestic point[10] using a Hewlett-Packard Agilent 8453 spectrophotometer under Kinetics mode with a cycle time of 0.5 s. Rate constants were obtained by fitting the Cc oxidation traces to monoexponential curves ($y = a \cdot e^{-b \cdot x} + c$ (MatLab; Mathworks)) after removal of the first five seconds during which concentrations fluctuated and signals were unstable. Multiple turnover rate constants were similarly obtained except with 1 µM CcP, 30 µM Cc, and 10 µM H_2O_2. An excess of Cc(Fe^{2+}) was used to minimize effects from depletion of the pool of reduced protein, as oxidized Cc also binds to CcP.

Solvent isotope effect on electron transfer rates

1 µM CcP and 1 µM Cc were combined in order to maintain the stability of CcP. The complex was diluted 500-fold into 100 mM KPi, pH 6 deuterium-based buffer overnight at 4 °C. Cc was fully oxidized by the following morning, so an additional 2 µM reduced Cc was added to the solution and brought up to a final volume of 1800 µL before initiating the reaction with 2 µM H_2O_2 at 20 °C with constant stirring (700 RPM). Parallel studies were conducted in protic buffer for direct comparison. Data were acquired and processed similar to single turnover measurements. Statistically significant differences were determined by a two-tailed Student's *t*-test assuming equal variances.

Crystallization of CcP:Cc complexes

CcP and Cc were combined in a 1:1 stoichiometric ratio and oxidized with potassium ferricyanide overnight. The CcP:Cc sample was exchanged into filtered Nanopure water and the final concentration was adjusted to 1 mM. Crystals of W191Y:L232E in complex with Cc formed in 2 μL hanging drops within a week (drops were mixed 1:1 with well solution: 100 mM sodium acetate, pH 5.4 – 6, 175 mM NaCl, 5 mM *n*-octyl-β-D-glucoside, 18% – 20% polyethylene glycol 3350). Crystals of W191Y:L232H in complex with Cc required 10 mM L-proline (Additive Screen HR2-428; Hampton) as a crystallization additive. The complex of WT CcP and Y48K Cc was crystallized in similar solutions from pH 4.6 – 5.0 and 14% – 20% polyethylene glycol 3350 without L-proline. Crystals were soaked briefly in 20% ethylene glycol as a cryoprotectant, flash frozen, and diffraction data were collected either at Cornell High Energy Synchrotron Source (CHESS) A1 beam line on an ADSC Quantum 210 CCD camera or at the NE-CAT Advanced Photon Source 24ID-C beam line on a PILATUS 6MF pixel array detector. All data were indexed, integrated, and scaled by HKL-2000. The structures were determined and refined by PHENIX[11]. Model building was performed with Coot[12]. The structures of the W191Y:L232E/H : WT Cc complex and the WT CcP : Y48K Cc complex were determined to ~2.9 Å and ~1.9 Å resolution, respectively, using molecular replacement with the parent W191Y:WT Cc and WT CcP:WT Cc structures as probes, respectively.

Electron spin resonance spectroscopy

CW-ESR: Compound I samples were prepared by combining 0.1 – 0.2 mM CcP and two molar equivalents of H_2O_2. The protein mixture was quickly loaded into an X-band ESR tube and flash frozen in liquid nitrogen within 30 seconds. Continuous-wave X-band spectra were acquired with a Bruker EleXSys II spectrometer at 9.39 GHz and 12 K with 100 kHz modulation frequency, 1 – 4 Gauss modulation amplitude, and 0.2 – 0.63 mW power. Power was varied to check for characteristic saturation effects of tyrosyl signals.

D_2O-treated samples were prepared by incubating 0.1 – 0.2 mM CcP in 100 mM KPi, pH 6 deuterium-based buffer overnight at 4 °C. Compound I was generated upon addition of two

molar equivalents of H_2O_2, quickly transferred to an X-band ESR tube, and flash frozen. A control sample in water-based buffer was prepared similarly to check for protein stability under identical conditions.

Rapid freeze quench experiments were carried out with a Bio-Logic SFM 300 machine that rapidly combines CcP samples with peroxide. As this method results in volume variations, instead of calculating a packing factor, an inert internal standard of Er:DTPA was added to the protein mixture. Er:DTPA was prepared by reacting a solution of 3 mM $Er_2(SO_4)_3 \bullet 8\ H_2O$ in 1 M HCl with 8 mM diethylenetriaminepentaacetic acid (DTPA; Sigma Chemical Company) in 0.1 M NaOH. The final pH was adjusted to 9. Samples containing 0.3 mM CcP, 1.5 mM Er:DTPA, and 0.6 mM Cc in 100 mM KPi, pH 6 were mixed with 0.6 mM H_2O_2, and after a set time delay, the mixture was sprayed into liquid ethane-filled glass funnels that were coupled to X-band ESR tubes with heat shrink tubing. The resultant snow was immediately packed with an aluminum rod by hand into the bottom of an ESR tube. Spectra were collected with a Bruker EleXSys II spectrometer at 9.39 GHz and 12 K with 100 kHz modulation frequency, 4 dB modulation amplitude, and 0.6325 mW power. Data were processed by MatLab and EasySpin[13].

The organic radical signal at g = 2 was isolated and corrected by subtracting a linear baseline. Cumulative numerical integration (`cumtrapz` followed by integration `trapz`) was then implemented. The Er:DTPA signal at g = 11.8 was similarly truncated, baseline corrected, and integrated with `trapz`. $Tyr^{\bullet}$ signals were normalized to those of Er:DTPA.

Averaged RFQ signals were fit to biexponential equations assuming a competitive reaction model (Equation 6) and rate constants were solved for by Equation 7[14,15]. For parent Y191 data, rate constants k_r and k_{obs} were iteratively solved. However, for Y191:E232 data, owing to the noise of the data set, k_{obs} was restrained such that the fit at 60 s was approximately equal to the averaged signal intensity between 15 s to 60 s, and k_r was assumed to be 0 s^{-1} given no observed decrease of the signal intensities over the time course of the experiment. A_0 was

measured by generating Y191 Cpd I RFQ samples without Cc using the same technique as described over similar time points (Table 1).

$$B(t) = \frac{A_0 k_f}{\gamma_2 - \gamma_1}\left(e^{-\gamma_1 t} - e^{-\gamma_2 t}\right) \quad (6)$$

$$\gamma_1 + \gamma_2 = k_f + k_r + k_{obs}$$
$$\gamma_1 \times \gamma_2 = k_r \times k_{obs} \quad (7)$$

ENDOR/ESEEM:

Samples of ~1 to 1.5 mM W191Y CcP and W191Y:L232E CcP were exchanged into 100 mM KPi, pH 6, 25% glycerol, D_2O-based buffer. After addition of peroxide to a final concentration of 3 mM, each sample was rapidly transferred to a Q-band quartz capillary tube (Wilmad LabGlass; L: 100 mm; OD: 1.6 mm; ID: 1.1 mm) and frozen in liquid nitrogen. Standards of L-tyrosine were prepared by dissolving 10 mM L-tyrosine in 12.5 mM sodium borate D_2O-based buffer, pD 10. Samples were frozen and irradiated for upwards of 15 m by a 36 W UV lamp at 77 K.

ENDOR and ESEEM spectra were recorded on a BRUKER Q-Band ElexSys E580 FT pulse EPR spectrometer equipped with a pulsed ENDOR ElexSys E560-P accessory and a ColdEdge cryogen-free cooling system. The temperature for the pulse experiments was maintained at 60K. Pulse ENDOR measurements were performed according to the Mims sequence with a variation of the tau time to compensate for blind spots. Three-pulse ESEEM data were processed using exponential baseline subtraction before the Fourier transform.

PCET thermodynamic and Brønsted analysis

Bond dissociation free energies (BDFE) were calculated following the delineated relation[16,17] using side chain acidities ($\Delta pK_a = pK_a(Tyr^{\bullet}) - pK_a(HB\text{-acceptor})$) and approximate CcP redox potentials relative to W191Y CcP ($E°$ in volts) with the appropriate coefficients to convert the calculated $\Delta\Delta G°' = \Delta G°'(\text{variant}) - \Delta G°'(\text{W191Y})$ into kcal mol^{-1} (Equation 4). Calculated BDFEs were compared to $-RT \ln(k/k_{W191Y})$, using rate constants from single turnover reactions. Scatterplots were fit with either a straight line to determine the slope α or were fit to Equation 8 to approximate $\Delta G°'_1$ and λ.

$$\Delta\Delta G^{\ddagger\prime} = \Delta\Delta G^{\circ\prime 2} + 2\lambda\Delta\Delta G^{\circ\prime} + 2\Delta G^{\circ\prime}{}_1\Delta\Delta G^{\circ\prime} \quad (8)$$

To assess the dependency on side chain pK_as, $\Delta\Delta$pK_a was fixed at 0 and BDFE values recalculated. The influence of the redox potential was evaluated in a similar manner.

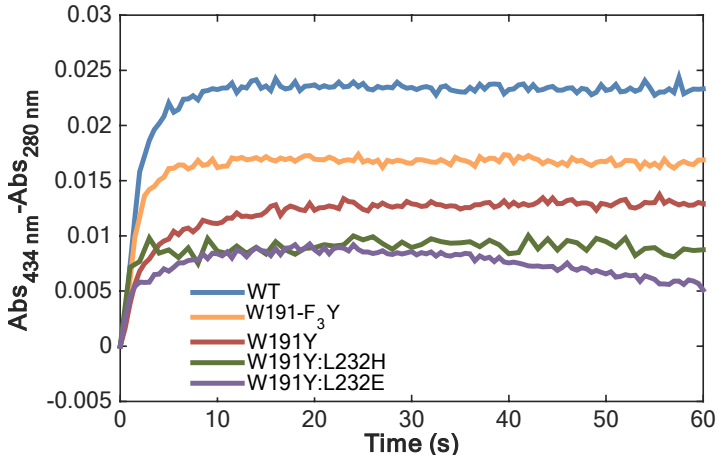

Supplemental Figure 1 – Progress curves for Cpd I formation. Reactions are shown for 1 µM CcP with 2 µM peroxide in 100 mM KP_i buffer, pH 6. CcP variants have similar rates of Cpd I formation but varying degrees of Cpd I stability, with the exception of W191Y:L2332E, which has somewhat reduced stability.

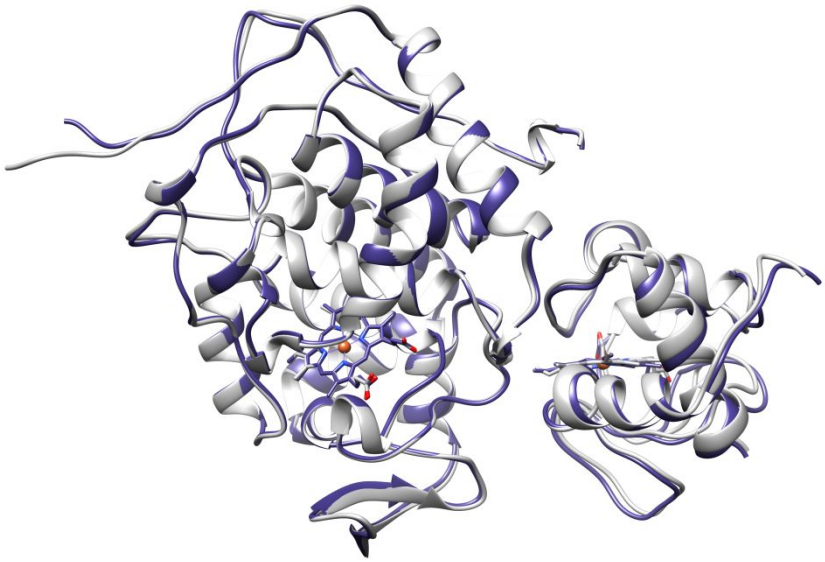

Supplemental Figure 2 – Crystal structure of WT CcP:CcY48K compared to that of WT CcP:WT Cc. Overlay of WT CcP:Y48K Cc (PDB 6P43; dark blue) and WT CcP:WT Cc (PDB 1U74; grey) shows no significant structural alterations between the two complexes.

Variant	pH	Single Turnover		Multiple Turnover	
		A	k_1 [s^{-1}]	*A*	k_1 [s^{-1}]
WT	6	0.043 ± 0.009	0.48 ± 0.09	0.58 ± 0.10	0.43 ± 0.06
WT + Y48K Cc	6	0.045 ± 0.009	0.45 ± 0.08	—	—
W191G	6	0.0224 ± 0.0014	0.0221 ± 0.0017	—	—
W191Y	6	0.021 ± 0.007	0.05 ± 0.02	0.66 ± 0.11	0.008 ± 0.003
W191Y + Y48K Cc	6	0.023 ± 0.009	0.042 ± 0.012	—	—
W191Y:L232E	6	0.044 ± 0.004	0.189 ± 0.006	0.101 ± 0.018	0.25 ± 0.04
W191Y:L232E	7	0.023 ± 0.002	0.101 ± 0.010	0.387 ± 0.017	0.028 ± 0.005
W191Y:L232E	8	0.0491 ± 0.0016	0.0128 ± 0.008	0.17 ± 0.04	0.0065 ± 0.0007
W191Y:L232E + Y48K Cc	6	0.046 ± 0.005	0.156 ± 0.005	—	—
W191Y:L232H	5	—	—	0.38 ± 0.02	0.0143 ± 0.0010
W191Y:L232H	6	0.022 ± 0.005	0.114 ± 0.016	0.325 ± 0.012	0.014 ± 0.004
W191Y:L232H	6.5	—	—	0.29 ± 0.04	0.037 ± 0.007
W191Y:L232H	7	0.028 ± 0.004	0.079 ± 0.014	0.37 ± 0.03	0.037 ± 0.005
W191Y:L232H	7.5	—	—	0.338 ± 0.018	0.027 ± 0.003
W191Y:L232H	8	0.040 ± 0.005	0.053 ± 0.008	0.206 ± 0.007	0.0092 ± 0.0012
W191(3,5)-F_2Y	6	0.0148 ± 0.0019	0.060 ± 0.015	—	—
W191(2,3,5)-F_3Y	6	0.022 ± 0.006	0.07 ± 0.02	0.554 ± 0.017	0.0149 ± 0.005
W191(2,3,5)-F_3Y:L232E	6	0.046 ± 0.003	0.132 ± 0.010	0.22 ± 0.05	0.107 ± 0.004
W191(2,3,5)-F_3Y:L232E	7	—	—	0.40 ± 0.02	0.024 ± 0.005

Supplemental Table 1 – Single and multiple turnover rate constants from reactions run in 100 mM KPi buffer. Constants were obtained by fits to a first-order decay model. Scalar coefficients *A* should ideally be ∼0.04 (single turnover; 2 µM Cc(Fe^{2+})) and ∼0.58 (multiple turnover; 30 µM Cc(Fe^{2+})), but owing to fluctuations in protein concentrations at early times and protein measurement variations, the first five seconds of the activity assays after mixing were omitted from some fits of the progress curves.

	W191YL232E:WT Cc	W191YL232H:WT Cc	WT:Y48K Cc
		Data Collection	
space group	$P2_1$	$P2_1$	P1
a, b, c (Å)	45.80, 112.07, 88.33	45.93, 111.92, 88.75	45.21, 50.89, 86.43
α, β, γ (deg)	90, 104.6, 90	90, 105.6, 90	105.65, 95.0, 107.31
no. of unique reflections	18509	17827	43661
resolution[a]	2.9/3.0 – 2.9	2.9/3.0 – 2.9	1.9/2.0 – 1.9
completeness (%)	95.9/78.2	83.7/45.9	76.8/65.2
$CC_{1/2}$	0.99/0.56	0.98/0.68	0.99/0.57
<I/σ>	10.9/0.6	6.7/0.6	12.6/1.5
R_{merge}[b]	0.175	0.164	0.076
		Refinement	
R_{work}[c]	23.7/40.1	21.2/34.6	19.1/24.5
R_{free}[c]	27.3/44.4	27.1/45.5	22.8/29.4
no. of atoms	6522	6528	6439
no. of water molecules	0	5	724
mean B value (Å^2)	89.5	68.1	25.5
B value (ligand) (Å^2)	94.8	69.6	15.7
B value (waters) (Å^2)	—	51.4	27.9
RMSD for bonds (Å)	0.004	0.007	0.005
RMSD for angles (deg)	0.95	1.05	1.05
φ/ψ stats (%)			
Ramachandran favored (%)	94.2	93.3	96.8
Ramachandran outliers (%)	0.00	0.3	0.4
Rotamer outliers (%)	0.7	0.5	0.8
Protein Data Bank entry	6P41	6P42	6P43

Supplemental Table 2 – X-ray diffraction data collection and structure refinement statistics. [a] Highest-resolution range for compiling statistics. [b] $R_{merge} = (\sum_i \sum_j |I_j - \langle I_i \rangle|)/[\sum_i (\sum_j I_j)]$, where I_j is the intensity of the *j*th observation of reflection *i*, $\langle I_i \rangle$ is the average intensity of reflection *i*, and N_i is the redundancy of reflection *i*. [c] R_{work} or $R_{free} = (\sum |F_{obs} - F_{calc}|)/(\sum |F_{obs}|)$.

Variant	$\Delta E^{\circ\prime}$ (V)	$\Delta\Delta pK_a$	$\Delta\Delta G^{\circ\prime}$	$\Delta\Delta G^{\circ\prime}$ ($\Delta E^{\circ\prime} = 0$)	$\Delta\Delta G^{\circ\prime}$ ($\Delta\Delta pK_a = 0$)
W191Y CcP + WT Cc	0	0	0	0	0
W191Y CcP + Y48K Cc	-0.10	—	2.31	0	2.31
W191Y:L232H CcP + WT Cc	0.10	-7.74	8.30	10.60	-2.31
W191Y:L232E CcP + WT Cc	0.20	-5.99	3.59	8.21	-4.61
W191Y:L232E CcP + Y48K Cc	0.10	-5.99	5.90	8.21	-2.31
W191(3,5)-F_3Y CcP + WT Cc	-0.025	-3.2	4.96	4.38	0.58
W191(2,3,5)-F_3Y CcP + WT Cc	0.039	-3.9	4.44	5.34	-0.90
W191(2,3,5)-F_3Y:L232E CcP + WT Cc	0.12	-9.89	10.79	13.55	-2.76
WT CcP + WT Cc	0.30	—	-6.92	—	-6.92
WT CcP + Y48K Cc	0.20	—	-9.22	—	-9.22

Supplemental Table 3 – Estimated thermodynamic parameters affecting PCET of Tyr191•. $\Delta\Delta G^{\circ\prime}$ (kcal/mol) was calculated as $\Delta\Delta G^{\circ\prime} = -23.06\ \Delta E^{\circ\prime} - 1.37\ \Delta\Delta pK_a$. The values for $\Delta\Delta pK_a$ were determined from literature values of amino acids in aqueous solution[6] relative to that of a hydronium ion, assuming that water accepts the proton in the case of W191Y; $\Delta E^{\circ\prime}$ (V) was approximated relative to that of W191Y CcP + WT Cc in 100 mM KP_i buffer, pH 6; and $-RT \ln (k/k_{W191Y})$ was calculated from single turnover rate constants in Supplemental Table 1. Dependency on PCET was assessed by either fixing $\Delta\Delta pK_a$ or $\Delta E^{\circ\prime}$ to 0.

References:

(1) Payne, T. M.; Yee, E. F.; Dzikovski, B.; Crane, B. R. Constraints on the Radical Cation Center of Cytochrome c Peroxidase for Electron Transfer from Cytochrome C. *Biochemistry* **2016**, *55* (34), 4807–4822.

(2) Pollock, W. B. R.; Rosell, F. I.; Twitchett, M. B.; Dumont, M. E.; Mauk, A. G. Bacterial Expression of a Mitochondrial Cytochrome c . Trimethylation of Lys72 in Yeast Iso-1-Cytochrome c and the Alkaline Conformational Transition. *Biochemistry* **1998**, *2960* (97), 6124–6131.

(3) DeWeerd, K.; Grigoryants, V.; Sun, Y.; Fetrow, J. S.; Scholes, C. P. EPR-Detected Folding Kinetics of Externally Located Cysteine-Directed Spin-Labeled Mutants of Iso-1-Cytochrome C. *Biochemistry* **2001**, *40* (51), 15846–15855.

(4) Vitello, L. B.; Huang, M.; Erman, J. E. PH-Dependent Spectral and Kinetic Properties of Cytochrome c Peroxidase: Comparison of Freshly Isolated and Stored Enzyme. *Biochemistry* **1990**, *29* (18), 4283–4288.

(5) Gil, A. A.; Haigney, A.; Laptenok, S. P.; Brust, R.; Lukacs, A.; Iuliano, J. N.; Jeng, J.; Melief, E. H.; Zhao, R. K.; Yoon, E. Bin; Clark, I. P.; Towrie, M.; Greetham, G. M.; Ng, A.; Truglio, J. J.; French, J. B.; Meech, S. R.; Tonge, P. J. Mechanism of the $AppA_{BLUF}$ Photocycle Probed by Site-Specific Incorporation of Fluorotyrosine Residues: Effect of the Y21 PK_a on the Forward and Reverse Ground-State Reactions. *J. Am. Chem. Soc.* **2016**, *138* (3), 926–935.

(6) Seyedsayamdost, M. R.; Reece, S. Y.; Nocera, D. G.; Stubbe, J. Mono-, Di-, Tri-, and Tetra-Substituted Fluorotyrosines: New Probes for Enzymes That Use Tyrosyl Radicals in Catalysis. *J. Am. Chem. Soc.* **2006**, *128* (5), 1569–1579.

(7) Minnihan, E. C.; Young, D. D.; Schultz, P. G.; Stubbe, J. Incorporation of Fluorotyrosines into Ribonucleotide Reductase Using an Evolved, Polyspecific Aminoacyl-TRNA Synthetase. *J. Am. Chem. Soc.* **2011**, *133* (40), 15942–15945.

(8) Matthis, A. L.; Vitello, L. B.; Erman, J. E. Oxidation of Yeast Iso-1 Ferrocytochrome c by Yeast Cytochrome c Peroxidase Compounds I and II. Dependence upon Ionic Strength. *Biochemistry* **1995**, *34* (31), 9991–9999.

(9) Miller, M. A. A Complete Mechanism for Steady-State Oxidation of Yeast Cytochrome c

by Yeast Cytochrome c Peroxidase. *Biochemistry* **1996**, *35* (49), 15791–15799.

(10) Miller, M. A.; Vitello, L.; Erman, J. E. Regulation of Interprotein Electron Transfer by Trp 191 of Cytochrome c Peroxidase. *Biochemistry* **1995**, *34* (37), 12048–12058.

(11) Adams, P. D.; Afonine, P. V.; Bunkóczi, G.; Chen, V. B.; Davis, I. W.; Echols, N.; Headd, J. J.; Hung, L. W.; Kapral, G. J.; Grosse-Kunstleve, R. W.; McCoy, A. J.; Moriarty, N. W.; Oeffner, R.; Read, R. J.; Richardson, D. C.; Richardson, J. S.; Terwilliger, T. C.; Zwart, P. H. PHENIX: A Comprehensive Python-Based System for Macromolecular Structure Solution. *Acta Crystallogr. Sect. D Biol. Crystallogr.* **2010**, *66* (2), 213–221.

(12) Emsley, P.; Lohkamp, B.; Scott, W. G.; Cowtan, K. Features and Development of Coot. *Acta Crystallogr. Sect. D Biol. Crystallogr.* **2010**, *66* (4), 486–501.

(13) Stoll, S.; Schweiger, A. EasySpin, a Comprehensive Software Package for Spectral Simulation and Analysis in EPR. *J. Magn. Reson.* **2006**, *178* (1), 42–55.

(14) Korobov, V.; Ochkov, V. *Chemical Kinetics with Mathcad and Maple*; Springer Vienna: Vienna, 2011.

(15) Bobrovnik, S. A. Determination the Rate Constants of Some Biexponential Reactions. *J. Biochem. Biophys. Methods* **2000**, *42* (1–2), 49–63.

(16) Mayer, J. M. Proton-Coupled Electron Transfer: A Reaction Chemist's View. *Annu. Rev. Phys. Chem.* **2004**, *55* (1), 363–390.

(17) Parker, V. D.; Handoo, K. L.; Roness, F.; Tilset, M. Electrode Potentials and the Thermodynamics of Isodesmic Reactions. *J. Am. Chem. Soc.* **1991**, *113* (20), 7493–7498.